Egypt. J. Chem. **Vol.** 68, SI: Z. M. Nofal, pp. 1085- 1097(2025)

Egyptian Journal of Chemistry

http://ejchem.journals.ekb.eg/

Sustainable Green Fuel Technology via Photocatalytic Desulfurization of Dibenzothiophene Under Visible Light Using Mixed Nanocomposite Catalyst

Asmaa S. Morshedy [1*], Rawan Mazen Abdelhamid[2], Gehan Safwat[2], N.H.Mohamed[1]

[1]*Egyptian Petroleum Research Institute, Nasr City, Cairo, Egypt*
[2]*Faculty of Biotechnology, MSA University, Cairo, Egypt*

Abstract

The growing desire for clean fuels and the severe standards for sulfur emissions have spurred the development of efficient and sustainable desulfurization processes. In the present work, a visible-light-driven mixed nanocomposite ($CuO@TiO_2$) was prepared and tested as a photocatalyst for the photo-degradation of dibenzothiophene (DBT), which is deleterious to the environment and the major sulfur-containing component of fossil fuels. The composite was synthesized by a facile process and characterized by XRD, FT-IR, Raman, BET measurements, SEM, EDX, UV–Vis diffuse reflectance spectroscopy (DRS), and PL. The visible-light-driven photocatalytic activity of mixed composite was higher than that of TiO_2 and CuO alone, due to the enhanced charge separation, the narrowed bandgap and the strong interaction between CuO and TiO_2 under visible-light irradiation. The photodegradation activity was markedly affected by the amount of catalyst, addition of oxidizing agent (hydrogen peroxide, H2O2) and irradiation time. A proposed mechanism indicated that superoxide and hydroxyl radicals were primarily responsible for DBT oxidation. The DBT removal under the optimum condition was 99.67%, while the real sample of diesel feedstock (1300ppm-Sulfur content) was 95.37% under LHL light and under Sun light was 98.92%. An extraction step was involved in the case of using real sample of diesel fuel to remove the oxidized sulfur compounds by using acetonitrile as solvent. Moreover, the catalyst showed high stability and reusability for six cycles, and could be a promising candidate to actual fuel desulfurization. This work provides a green, efficient and low-cost approach for the preparation of ultra-low sulfur fuel based on solar energy.

Keywords: Dibenzothiophene (DBT); Fuel desulfurization, Ultra-low sulfur fuel, Nanocomposites, Visible light.

1. Introduction

The continuous increase in the global population and rapid expansion of economic activities has led to an extraordinary surge in energy demand, especially for naturally available and cost-effective fuel oil [1, 2]. However, crude fuel oil contains various cyclic sulfur compounds, such as thiophene, benzothiophene and dibenzothiophene, which are the main factors of SOx in emissions in the combustion process, and leads to serious problems in environment pollution [3, 4]. Therefore, it is necessary to have efficient desulfurization processes, especially for petrochemical industries [5]. The use of photocatalysis for environmental purification is primarily for the desulfurization of fuel [6, 7]. Although traditional HDS technologies are commonly used in refineries, they need high temperature/pressure and intensive hydrogen consumption, which cannot be ignored due to the economic and operation pressures [8]. Other options for desulfurization such as extractive [9], oxidative [10], adsorptive [11], and biological processing techniques have been considered [12]. Among them, oxidative desulfurization (ODS) is a notable process due to its efficiency and economic accessibility and in particular, its capacity to eliminate recalcitrant sulfur compounds in the presence of oxidant agents (e.g., hydrogen peroxide) [13, 14]. Photocatalytic oxidative desulfurization in particular is very promising because it produces highly-oxidizing species like hydroxyl radicals (•OH) that leads to the cleavage of sulfur compounds [15-17]. The semiconductor photocatalysts are of great concern for their high efficiency in the accessible longer wavelength (800 nm) light source. The photo-oxidation property and catalytic activity of these photocatalysts are proved to be higher than that of other existing materials [18, 19]. Metal oxides have received great attention due to their excellent photochemical properties for photodesulfurization. The role of oxygen vacancies in the template synthesis of metal oxides and the synergetic effects of binary as well as ternary oxides have been found to be especially important. Such enhanced charge separation and broadened light absorption features made them to be promising candidates for the photocatalytic desulfurization process. Mixed metal oxide nanocomposites are among them and have received much interest due to its abundant stability, and excellent light-harvesting ability [20, 21]. Furthermore, it owns highly catalytic properties and is easy to be separated and recycled such that it can be reused.

Ideal photocatalyst for applications like photodesulfurization should satisfies: (1) stability in light irradiation conditions, (2) resistant to biological and chemical decomposition and (3) lower in cost (4) interact better with the reactants under appropriate excitation photon [6, 22].

*Corresponding author e-mail: E-mail addresses: Asmaa_Morshedy@epri.sci.eg (Asmaa S. Morshedy).
Received date 03 May 2025; Revised date 21 June 2025; Accepted date 25 June 2025
DOI: 10.21608/ejchem.2025.381331.11685
©2025 National Information and Documentation Center (NIDOC)

In the present work, mixed composite of ($CuO@TiO_2$) was successfully prepared and showed remarkable photocatalytic performance toward dibenzothiophene (DBT), one of the most prevalent sulfur-containing impurities that occur in diesel fuel due to the synergetic effect at the interface and efficient visible light absorption. The innovation of the present work is the specially prepared mixed metal oxide as a nanocomposite photocatalyst for the degradation of DBT, and p-n heterojunction formation between CuO (p-type semiconductor) and TiO_2 (n-type semiconductor) can result in efficient photo-generated charge separation, reducing the electron-hole recombination and hence improving the efficiency of the photocatalyst. In many catalytic reactions, TiO_2 has been used as a co-catalyst or promoter of an active phase. As a visible-light- active and stable photocatalyst, CuO/TiO_2 would be very attractive material for sulfur-removal under visible light irradiation. As its notable feature of reusability and stability, the mixed photo-catalyst could be recycled. This work presents a sustainable, green and low cost approach of solar-driven synthesis of ultra-low sulfur fuels for environmental and clean energy applications.

2. EXPERIMENTAL

2.1 Materials and techniques

All chemicals were analytical grade and were purchased from Sigma-Aldrich, and were used as received without further purification.

Titanium tetrachloride ($TiCl_4$, 99%) was purchased from Merck (Germany), hydrochloric acid (HCl, 36%) from Sigma-Aldrich (Germany), copper(II) nitrate trihydrate [$Cu(NO_3)_2 \bullet 3H_2O$, 99%] from Sigma-Aldrich (Germany), and ammonium hydroxide (NH_4OH, 33%) from Sigma-Aldrich (Germany). All reagents were of analytical grade and were employed without further purification. Diesel feedstock, obtained from Middor feedstock, Egypt, has been employed for this study.

Table (1): Characterizations for Middor diesel feedstock

Characterization	Diesel feedstock	ASTM Code
Yield, Wt. %.	100	-
Refractive index,20 ^oC	1.4668	D-1218
Density, 20 ^oC, gm/cm^3	0.8267	D-1298
Sulfur content, ppm	1300	D-4294
Aniline point, ^oC	70.4 (158 ^oF)	D-611
Diesel index	**52.20**	-

2.2 Synthesis

2.2.1 Preparation of mixed nanocomopsite catalyst

First, the preparation of copper oxide (CuO NPs) catalyst via the co-precipitation method. A 0.05 M solution of copper(II) nitrate trihydrate was prepared using a mixed of water (distilled) and stirred at 70°C for 30 min in order to guarantee that the dissolution is complete. Ammonium hydroxide (NH_4OH) was then added to the solution as a precipitating agent dropwise until pH of the solution was about 11. Then, the reaction mixture was stirred at room temperature for an extra 60 min to ensure the full formation of copper hydroxide (brown precipitate). The precipitate was collected by settling, and washed well with deionized water to remove ions before filtering. The resulting solid was dried in an oven at 120 °C for 6 h. Finally, the obtained dried copper hydroxide was calcined in a muffle furnace at for 4 hr at 500°C to form pure crystalline copper oxide (CuO) nanoparticles **Catalyst A**.

Secondly, the preparation of TiO_2 NPs (**Catalyst B**). Anatase-phase TiO_2 nanoparticles were prepared according to the authors' previous work [23]. In short, pre-cooled titanium tetrachloride ($TiCl_4$) was slowly diluted into hydrochloric acid to form a colorless solution. This solution was then poured into 1 M aqueous ammonia at 25°C with stirring. To obtain the desired anatase TiO_2, the resultant precipitate was dried in an oven at 120°C for 6 h and further calcined at 500°C for 4 h [24].

Finally, $CuO@TiO_2$ nanocomposites (**Catalyst C**) was prepared by facile physical mixing method. equimolar quantity of CuO was mixed with TiO_2 powder and then manually ground in a mortar to get good dispersion. The mixtures were then sonicated for 60 min at 50°C to promote interaction among the constituents and the uniformity of the mixtures.The sonicated mixture were dried to yield the final mixed nanocomposite with well dispersion.

2.3 Characterization Techniques of Photocatalyst

The as-prepared photocatalysts were characterized by a series of characterization methods. The crystallinity was identified by X-ray diffraction (XRD) with a Shimadzu XD-1 instrument using Cu-Kα radiation (λ = 0.154 nm). The functional groups of the composites were detected by FTIR instrument (Perkin Elmer) with standard KBr pellet. Raman spectra detected utilized a BRUKER 110/S spectrometer in the range from 150-4000 cm−1. The surface morphology and elemental composition were determined by scanning electron microscopy (SEM, Quanta-250 FEG, FEI, the Netherlands) with energy dispersive X-ray spectroscopy (EDX).

UV–vis DRS spectra were obtained from 200 to 800 nm using a Jasco V-570 spectrophotometer equipped with a Shimadzu IRS-2200 diffuse reflectance accessory. The photoluminescence (PL) properties were measured at room temperature using a spectrofluorometer (JASCO FP-6500, Jasco International Co., Ltd., Tokyo, Japan) with an excitation wavelength of λ = 250 nm. The Brunauer–Emmett–Teller (BET) surface area and porosity were characterized by nitrogen adsorption–desorption isotherms at −196 °C with a Quantachrome Nova 3200e analyzer, after degassing the samples at 300 °C for 6 h under vacuum (1.3×10^{-3} Pa). Photodesulfurization studies of the degradation of dibenzothiophene (DBT) was monitored by reversed-phase high-performance liquid chromatography (RP-HPLC) (C18: 250 × 4.60 mm, 5 μm). The mobile phase was a 55:45 (v/v) mixture of water and acetonitrile at a flow rate of 0.8 mL/min and detection at 230 nm.

2.4 Photocatalytic Activity Measurements

The desulfurization of the DBT was performed in 20 mL of the sample with 0.1 g of the catalyst under light sources, of visible light using a line halogen lamp (550 nm, 500 W) in a double-jacketed quartz reactor for a maximum 90 min. The adsorption properties of the prepared catalysts were evaluated in the dark by placing 0.1 g of the catalyst to 20 mL of the feed for 24 h before irradiation. A number of factors were studied in the present research, such as the source of light, amount of catalyst, time of irradiation, and the effect of oxidizing agent (hydrogen peroxide). The optimum conditions are performed for diesel feed stock 1300 ppm. Finally, the role of sun irradiation was studied at the optimum conditions.

3. Results and discussions

3.1 Characterizations

3.1.1 XRD analyses

The structural properties of pure TiO_2 (**Catalyst A**), CuO (**Catalyst B**) and Mixed nanocomposite were examined using X-ray diffraction (XRD), as illustrated in **Figure 1a**. The XRD spectrum for pure TiO_2 revealed prominent peaks at 2θ angles of 25.31° (101), 38.02° (004), 47.84° (200), 55.07° (105), and 62.84° (204), which correspond to the anatase phase of crystalline TiO_2 [23]. While, CuO showed peaks at 2θ angles of 32.51° (110), 35.56° (002), 38.84° (111), 48.72° (202), 53.48° (020), 58.35° (202), 61.53° (113), 66.05° (311), and 68° (200), aligning with the crystalline planes of CuO (**Catalyst B**). Furthermore, in **Mixed nanocomposite** sample, all peaks of both CuO and TiO_2 were detected in XRD of the nanocomposite, affirming the successful preparation of the nanocomposite. In addition, the absence of any extra impurities peaks indicates that the as-prepared **Mixed nanocomposite** was effectively produced with high purity and crystallinity [24].

3.1.2 Infra-red measurements

Fourier-transform infrared (FTIR) spectroscopy of as-prepared samples was illustrated in **Figure 1b**. For catalyst A, (pure TiO_2) highlighted two key regions: 450-850 cm^{-1} and 3000-3700 cm^{-1}. The broad peak in the 450-850 cm^{-1} range corresponds to the stretching vibrations of TiO_2 [25, 26]. Meanwhile, the peak observed in the 3000-3500 cm^{-1} range is attributed to the OH stretching vibrations of surface hydroxyl groups. For the Mixed nanocomposite, notable peaks were found around 520 cm^{-1} and 595 cm^{-1}, which are indicative of Cu-O stretching vibrations [27, 28].

3.1.3 Raman spectroscopy

Raman spectroscopy provided detailed insights into the structural characteristics of pure TiO_2 & CuO, and its **Mixed nanocomposite**, as shown in **Figure 1c**. All samples displayed a prominent peak at 151 cm^{-1}, corresponding to the E(g) mode, which indicates the symmetric stretching vibrations of O–Ti–O bonds in TiO_2 (Catalyst A) [25, 29]. Notably, the intensity of this 151 cm^{-1} peak presented for CuO (Catalyst B). For the Mixed nanocomposite, the combination of the two catalysts highlights the substantial impact of CuO doping on the TiO_2 lattice. Such structural modifications influence the material's physical and chemical properties, potentially leading to enhanced catalytic performance [24].

3.1.4 Surface area and pore size distributions

N2 adsorption–desorption measurements were carried out for both pure TiO_2, CuO, and **Mixed nanocomposite** as depicted in **Figure 1d**. The isotherm for pure **Catalyst A** (TiO_2), **Catalyst B** (CuO), and Mixed nanocomposite showed a Type IV curve, typically for mesoporous materials, and featured a distinct H1-type hysteresis loop within the relative pressure range of 0.6 to 1.0, suggesting the presence of well-defined mesoporous structures [23]. The BET specific surface area was determined to be 110.15 m^2/g for pure TiO_2, 55.36 for pure CuO, and 90.47 m^2/g for the Mixed nanocomposite. This reduction in surface area with the combination of TiO_2 with CuO suggests some degree of pore occupation by the CuO nanoparticles [23]. Additionally, The BET specific surface area, pore volume, and average pore diameter for three samples are presented in **Table 2**.

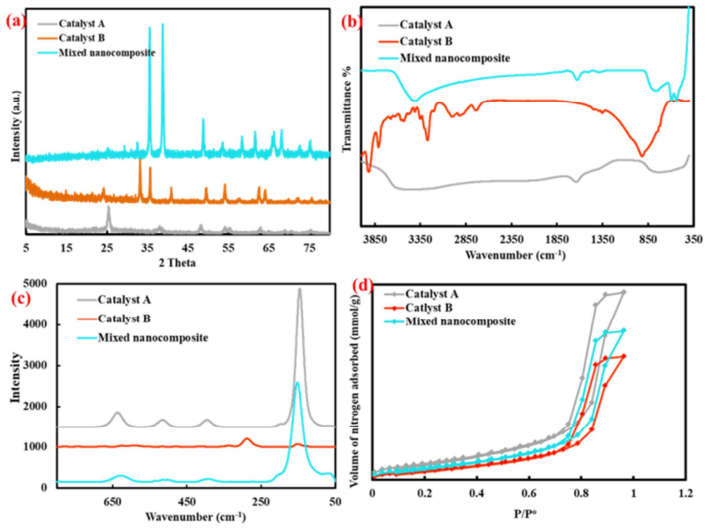

Fig. 1: (a) XRD of the prepared Catalyst A (TiO_2), Catalyst B (CuO), and Mixed nanocomposite, (b) FTIR of the prepared samples, (c) Raman spectroscopy, and (d) The N_2 adsorption-desorption isotherms

Table (2): The specific surface area, pore volume, and average pore diameter of three catalysts.

Catalyst	Surface area (m^2/g)	Pore volume (cm^3/g)	Average pore diameter (nm)
Catalyst A	110.15	0.273	6.529
Catalyst B	55.36	0.150	4.127
Catalyst C	90.47	0.261	3.743

3.1.5 Morphological studies

To examine the composite's morphology in greater detail, a SEM with an EDX analysis study was carried out. **Figure 2a** shows the typical (inset) SEM image of the composite. SEM image of **Mixed nanocomposite** illustrate the shape of extremely fine drops and spheres with little agglomerates on the surface of TiO_2 Nps.

Moreover, **Figure 2b** demonstrates the EDX spectrum of as-prepared **Mixed nanocomposite**. The peaks show that essential elements present (Cu, Ti, and O). The absence of any other atoms ensures the high purity of the as-prepared **Mixed nanocomposite** and this is in accordance with the XRD peaks, since, it is free from unknown peak in the XRD pattern.

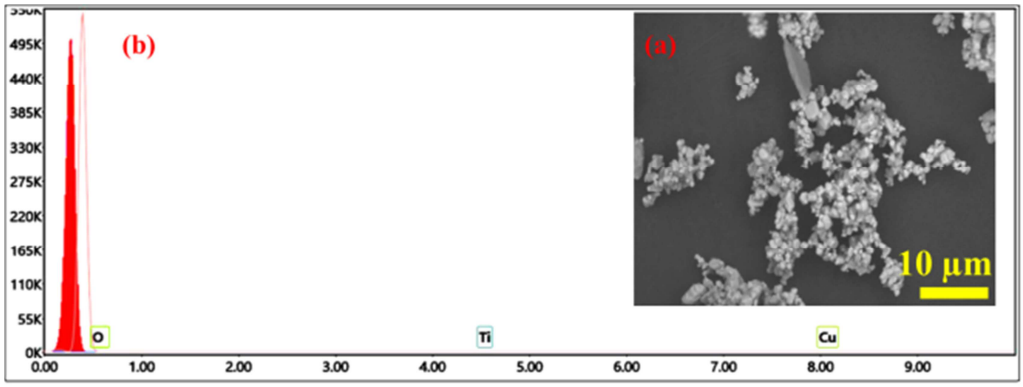

Fig.2: (a) In set SEM image & (b) EDX of the prepared Mixed nanocomposite.

3.1.6 Optical studies

The optical behavior of **Catalyst A (TiO_2), Catalyst B (CuO), and Mixed Nanocomposite** was studied via UV-visible diffuse reflectance spectroscopy, as illustrated in **Figure 3(a-c)**. CuO displayed an absorption band at 550 nm and TiO_2 at 385 nm [30, 31]. While, **Mixed nanocomposite** showed strong absorption in the visible light region, with notable peaks at 460 nm. The UV-vis spectra indicate that the incorporation of CuO into the TiO_2 exhibits a red significant absorption in the visible spectrum, with the absorption edge shifting to longer wavelengths, suggesting its potential for superior photocatalytic performance under visible light conditions [32].

The band gap energies of the three samples were determined from their optical absorption spectra using Tauc's Equation (eq.1):

$$(\alpha h\upsilon)^n = A(h\upsilon - Eg) \qquad \text{eq.(1)}$$

Where α is the coefficient of absorption, hυ is photon energy, A is a constant, and Eg is the optical bandgap, respectively. As shown in **Figure 3(d-f)**, the calculated band gaps for the **Catalyst A** (Pure TiO_2), **Catalyst B** (Pure CuO), and Mixed nanocomposite were 3.2, 2.2 and 2.6 eV, correspondingly. This reduction in band gap enhances the materials' ability to absorb visible light, indicating their potential as effective photocatalysts for photodesulfurization process.

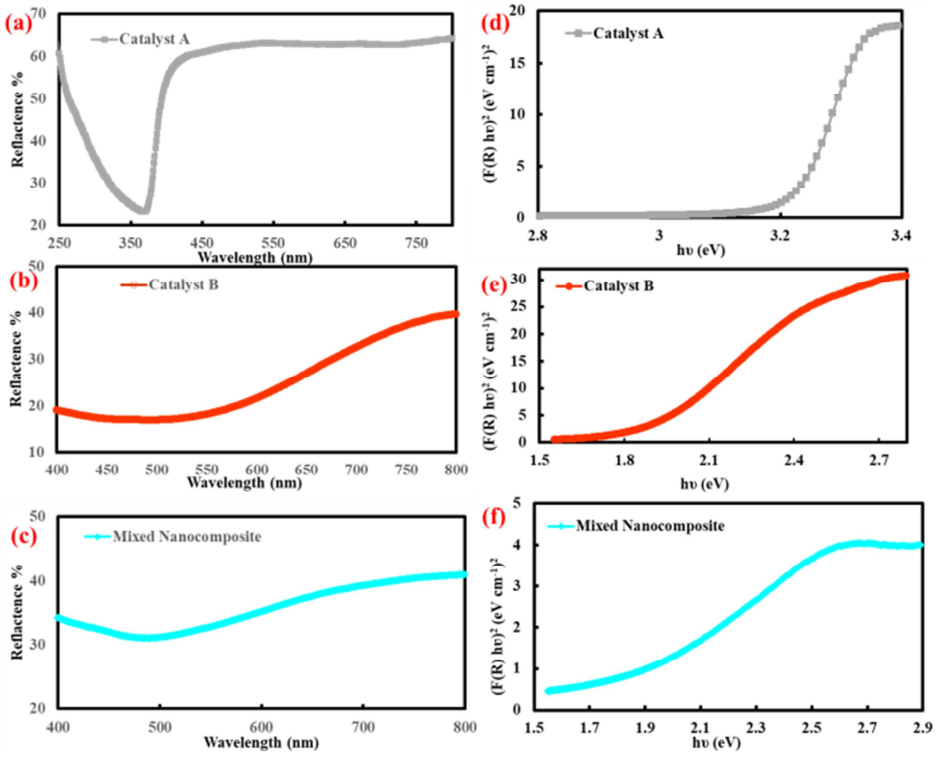

Fig. 3: (a-c) Uv- Visible reflectance & (d-f) Bandgap of the as-prepared samples.

3.1.7 Photoluminescence Spectroscopy

The charge migration and transfer performance of the synthesized samples were evaluated through photoluminescence (PL) spectra analysis. Generally, photocatalysts are designed and utilized to enhance photocatalytic efficiency by minimizing electron-hole recombination rate, as the rapid recombination of electrons and holes is a key limitation in photocatalysis. PL intensity is directly related to the recombination rate of photo-induced charge carriers, where higher PL intensity under light irradiation indicates a greater rate of electron-hole recombination [32].

Figure 4 presents the PL spectra of the three samples and the intensity decreases in the following order: **Catalyst B > Catalyst A > Mixed nanocomposite**. Since, **Mixed nanocomposite** shows the lowest PL intensity so, this may be an efficient electron migration from **Catalyst B** (CuO) reduces the recombination of photogenerated electron-hole pairs in the **Mixed nanocomposite**. This finding indicates that the **Mixed nanocomposite** can extend the photocatalytic excitation state, leading to a longer half-life. Also, improves carrier separation, it could lead to a higher desulfurization rate under visible light, making it more efficient for sustainable energy generation.

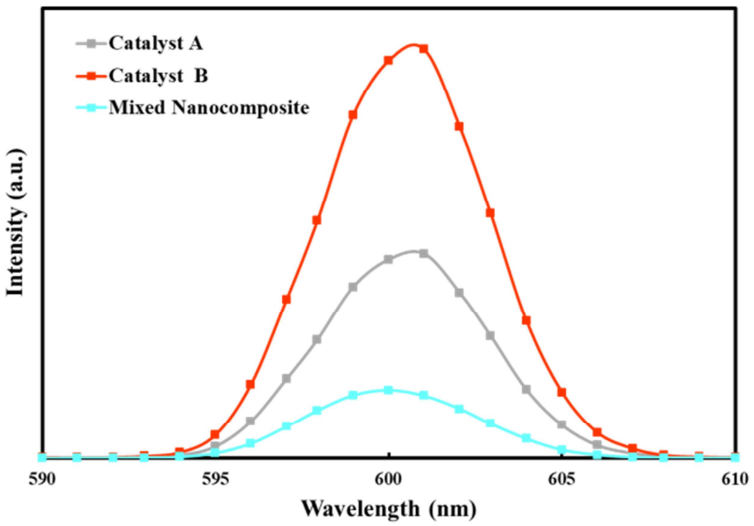

Fig. 4: PL spectroscopy of the as-prepared Samples.

4.1 Photodesulfurization process

4.1.1 Experiments in the dark

Prior to the photocatalytic process, the generated nanocomposites' adsorption capacities towards sulfur compounds were evaluated in the dark for 24 hours. The data are graphically represented in Figure 5, where **Catalyst A**, with a surface area of (110 m2g-1), demonstrated the best adsorption capability towards S removal (20%) in comparison to **Catalyst B** (11%) and **Mixed nanocomposite** (17.5%).

Contrary to the adsorption results, **Mixed nanocomposite** showed the highest photocatalytic desulfurization (39%) of DBT removal under the influence of LHL 550nm, 500W for 60 min., and one gram per liter due to its suitable band gap energy (2.6 eV) and prolonged photocatalytic performance due to lower electron/hole pair recombination as previously detected by PL measurements (**Figure 5**). The impact of various operational factors on the photo-desulfurization of DBT was thus investigated using **Mixed nanocomposite** in this study.

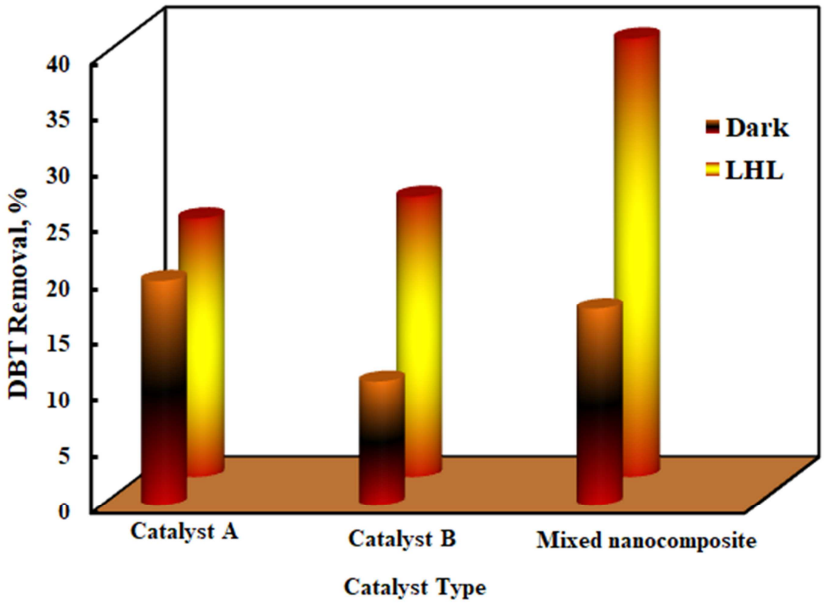

Fig. 5: Effect of Dark and LHL (500W) light of as-prepared samples on photodesulfurization process. (Conditions: dose= (1g/L), time= 60 min.).

4.1.2 Effect of amount of catalyst

Figure 6 shows how the catalyst dosage (0.25-2 g/L) affected the photo-desulfurization process for 1 hour under LHL lamp light. The amount of DBT removed rose consistently as the catalyst/DBT ratio grew from 0.25 to 1 g/L (39%). The total photocatalytic activity, however, decreased to 22% when the catalyst/feed ratio was above 1.75g because the other catalyst particles unintentionally scattered light [33].

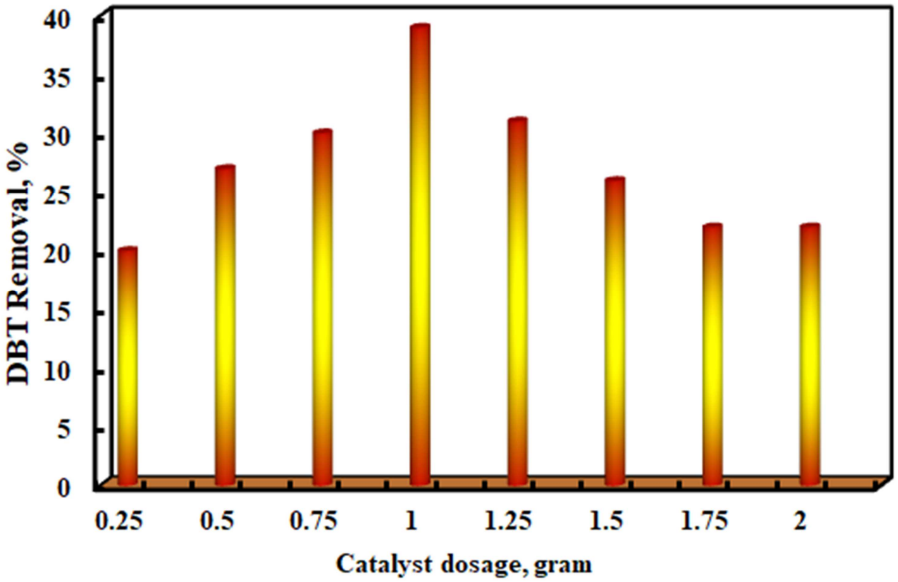

Fig. 6: Effect of Catalyst dose on the DBT removal%. (Conditions: dose= (0.25-2 g/L), time= 60 min., LHL).

4.1.3 Effect of oxidizing agent H_2O_2 insituo with DBT

The use of an oxidizing agent, H_2O_2, to oxidize DBT in the presence of **Mixed nanocomposite** catalyst was another factor in this section. The process was performed using the optimum condition of Mixed nanocomposite,s dose 1g/L for one hour under LHL.

Figure 7 shows the effect of addition technique of H_2O_2 to the photocatalytic process of DBT removal. This finding may encourage the use of **Mixed nanocomposite** photocatalyst as a practical and highly effective photocatalyst for a variety of environmental management applications. And the best ratio of DBT/ H_2O_2 was (1:0.75) volume by volume and the DBT removal recored nearly 99.67%.

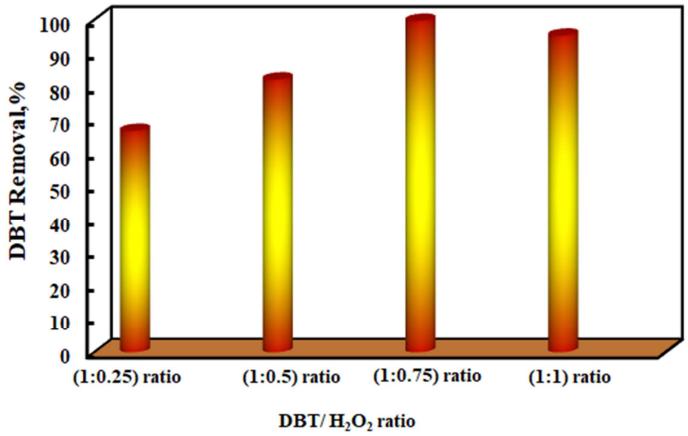

Fig. 7: Effect of DBT/H_2O_2 ratio on DBT removal%.

4.1.4 Effect of time

After obtaining the optimum condition of catalyst type, dosage and addition of hydrogen peroxide, **Figure 8** shows the effect of contact time (15, 30, 45, 60, 75, 90) minutes at these conditions. A maximum DBT of 99.67 % after 60 min. on contrast, by increasing the time there is any progress in the photo-desulfurization process.

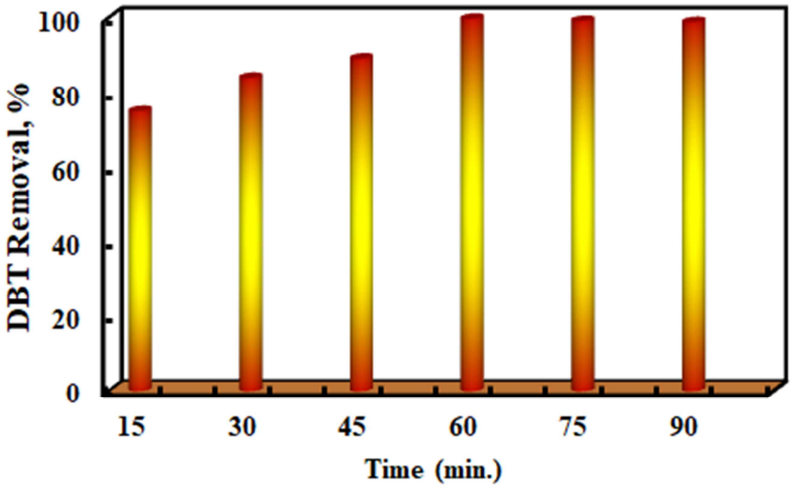

Fig. 8: Effect of the contact time on sulfur removal%.

4.1.5 Effect of Sunlight

The goal of this stage was to reduce the process costs by replacing the LHL with sunlight irradiation at the last optimum operating factor and applying the obtainable optimum conditions on a real feed stock of diesel fuel with sulfur content of 1300 ppm. According to Morshedy and his co-workers [34], the average intensity of sunlight in Egypt at the time of the tests was 1371 W/m^2. **Figure 9** shows the sulfur removal % was reached up to 99% under sunlight at the optimum conditions compared to artificial LHL (95.37%) under the same conditions. In this stage a solvent extraction step was involved for the removal of the oxidized products of sulfur compounds via using acetonitrile CH_3CN and the Solvent to feed (S/F) ratio was 2:1. In terms of economics and energy consumption, an economic desulfurization reaction to produce ultra-clean diesel fuel utilizing **Mixed nanocomposite** of ($CuO@TiO_2$) can be achieved.

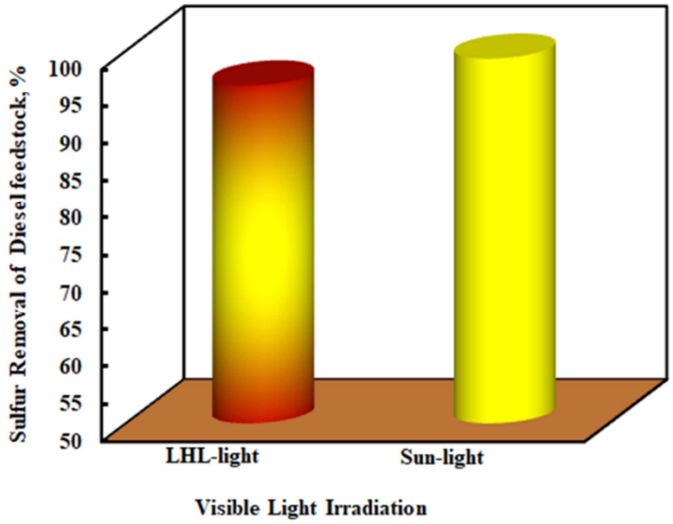

Fig. 9: Effect of the Sunlight irradiation on sulfur removal%.*Conditions: dose (1g/L), time (60 min.), Diesel feed/H_2O_2 ratio (1:0.75), and CH_3CN to feed ratio (2:1).

4.2 Recycling process

Recyclability of the catalyst is crucial for industrialization. At ideal conditions, the photo catalyst could be used more than seven times while retaining excellent photocatalytic activity, as shown in Figure 10a. Additionally, to further support the synthesized nanocomposite's endurance, we contrast the XRD pattern of the used catalyst (Figure 10b). The strong interaction between CuO and TiO_2 and the great stability of the photocatalyst were provided by the catalyst, which was shown by the XRD pattern to have retained its structural and compositional integrity during the recycling runs.

Figure 10a shows the catalyst may be used more than six times to desulfurize diesel oil without losing any of its exceptional photocatalytic activity. Also, the extraction capacity of the solvent used may be created and used repeatedly without losing its effectiveness; the approach offers a high long-term viability for practical applications.

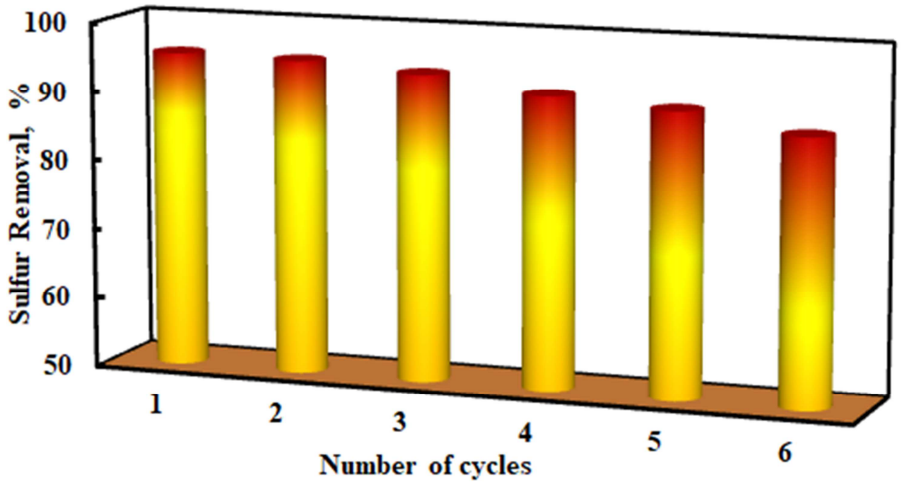

Fig. 10a: Catalyst recycling on photo desulfurization process.

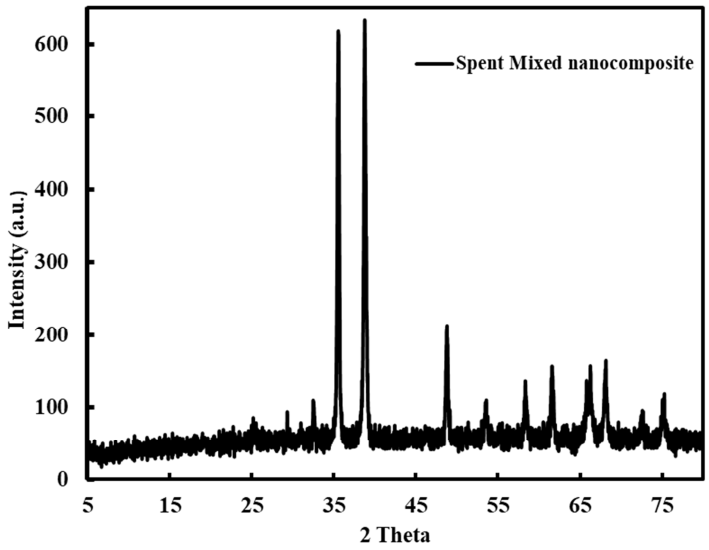

Fig. 10b: XRD of spent Mixed nanocomposite ($CuO@TiO_2$).

4.3 Mechanism of photodesulfurization process

One such hypothetical mechanism is shown in **Figure 11**. When photo-catalyst is irradiated, photons are absorbed and the electrons transfer from the VB to the CB, resulting in positive holes in the VB serving as the oxidant according to Eq. 2. The Mixed nanocomposite has a high PL character that reinforces the inhibition of the recombination of photo-excited electron–hole couples and contribution toward the photoexcited charge carrier's separation. This delayed recombination allows holes to migrate to the catalyst surface, where they can efficiently oxidize organic sulfur compounds as represented by Eq. 3. Moreover, with the introduction of H_2O_2, desulfurization efficiency is improved via generation of highly reactive hydroxyl radicals, and furthermore via deters h^+/e^- from recombining (Eq. 4). Hydroxyl radicals considered as a powerful oxidizing agent who oxidized the sulfur compounds to the corresponding sulfone and sulfoxide, which can be removed easily by solvent extraction step as shown in Eq. 5&6.

These results indicate that an integration of photocatalytic and photochemical oxidation processes can effectively enhance the removal efficiency of sulfur.

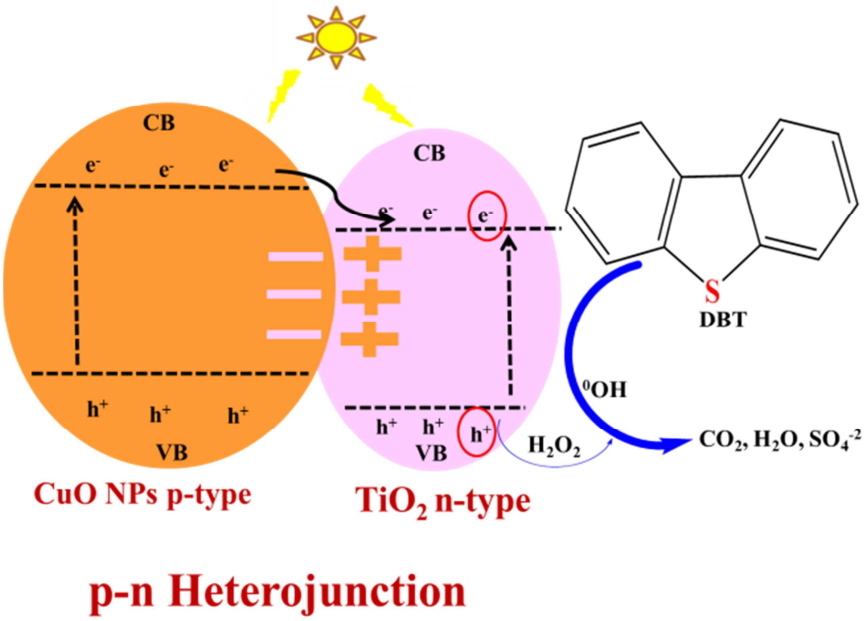

Fig.11: Systematic diagram for the photocatalytic desulfurization process.

Mixed nanocomposite+ hU→(hole)$^{+}$+(electron)$^{-}$ Eq. (2)

Mixed nanocomposite (h^{+})+ Sulfur →Mixed nanocomposite+ Oxidation product Eq. (3)

H_2O_2 + hv → 2 $^{\bullet}$OH Eq. (4)

Mixed nanocomposite(e^{-})+ H_2O_2 → 2 •OH Eq (5)

2$^{\bullet}$OH + Sulfur compounds → CO_2+H_2O+SO_4^{-2} Eq (6)

Since CuO is considered as P-type semiconductor [35, 36] and TiO_2 is n-Type [37, 38] So, the **Mixed nanocomposite** of them these produce P–N heterojunction which is critical to the separation and transport of photo-excited carriers. The heterojunction excellent in reducing recombination loss and promoting effective charge transfer region would substantially improve the photocatalytic activity of the composite, indicative of high potential for future photocatalytic applications [39].

4.4 Comparative evaluation of photocatalytic desulfurization efficiencies of Mixed nanocomposite versus other from recent publications

Photocatalytic desulfurization is a rapidly developing area, with several catalysts being created to efficiently utilize solar energy. **Table 3** compares different catalysts, light sources, and Sulfur removal. This research found that the ($CuO@TiO_2$) Mixed nanocomposite gave up to 99% removal for DBT model compound of 500 ppm, 95.37% for diesel feedstock under LHL of 550nm&500W. On the other hand, under sun light, the sulfur removal reached over 98% for real sample diesel feedstock. This data exceeds that of other state-of-the-art catalysts, offering a foundation for future investigations into the development and optimization of analogous nanocomposite systems to achieve superior photocatalytic desulfurization performance.

Table (3): Comparison of diferent catalysts for photodesulfurization process

Photocatalyst	Conditions	Sulfur Removal, %	References
Cu–ZnO/TiO_2	Dibenzothiophene (DBT), (BT), (T), model fuel in n-hexane solvent (500 ppm), oxidant: H_2O_2 (30%), light source: 500 W Xe-lamp	88.12	[40]
Cu-doped TiO_2/$BiVO_4$	DBT in model fuel; H_2O_2; visible light >500 nm	93	[41]

Au-m-TiO_2/g-C_3N_4	Dibenzothiophene (DBT), model fuel in n-octane (500ppm), oxidant: H_2O_2 , visible light >400 nm	98.7	[42]
Ultrasonically synthesized TiO_2	Thiophene, oxidant: H_2O_2, UV light	43 (toluene); 100 (n-hexane, n-octane)	[43]
Amorphous TiO_2 in ionic liquid	DBT, BT, 4,6-DMDBT, RSH, oxidant: H_2O_2, UV light, optimal reaction conditions	96.6	[44]
$H_5PV_2Mo_{10}O_{40}/TiO_2$	4-Methyldibenzothiophene (4-MDBT), oxidant: H_2O_2, temperature: 60°C, UV light	99.0	[45]
HY@TiO_2-1.5	DBT, BT, oxidant: H_2O_2, temperature: 70°C, UV light	99.7 for DBT, 85.0 for BT	[46]
Tl-doped TiO_2 Nanofibers	Diesel fuel, oxidant: H_2O_2, light source: Xe lamp.	98.74	[47]
Mixed nanocomposite (CuO@TiO_2) NPs	DBT, 500 ppm Diesel fuel (1300 ppm), oxidant: H_2O_2, light source: (LHL lamp, Sun).	99.67 95.37 (LHL)& 98.92 (Sun)	**This Work**

5. Conclusions

In the present work, a visible-light-driven mixed photocatalyst (CuO@TiO_2) was successfully prepared and showed remarkable photocatalytic performance toward dibenzothiophene (DBT) degradation, one of the most prevalent sulfur-containing impurities that occur in diesel fuel. The characteristic properties of the the three catalysts were confirmed by XRD, SEM-EDX, FTIR, Raman spectroscopy, Uv reflectance and photoluminace spectra. From the data, the three nanocomposites were found to be effective under visible light (LHL, 550nm, 500W). Mixed nanocomposite had lowest the PL recombination rate and showed the highest activity. The boosted activity over the pure catalysts (CuO or TiO_2) was due to improved separation of charges, synergetic effect at the interface and efficient visible light absorption. The photocatalytic performance was also affected by catalyst amount, H_2O_2 dosage, and irradiation time, where the superoxide and hydroxyl radicals were the main radicals along the degradation route. Under optimal conditions, the removal efficiency of DBT reached 99.67%. When applied to a real diesel feedstock sample containing 1300 ppm of sulfur, the desulfurization efficiency was 95.37% under laboratory halogen lamp (LHL) illumination and 98.92% under natural sunlight. For the real diesel sample, an additional extraction step was implemented using acetonitrile as the solvent to separate the oxidized sulfur compounds. Furthermore, the catalyst demonstrated excellent stability and reusability over six consecutive cycles, indicating its strong potential for practical applications in fuel desulfurization. As its notable feature of reusability and stability, the mixed photocatalyst could be recycled. This work presents a sustainable, green and low cost approach of solar-driven synthesis of ultra-low sulfur fuels for environmental and clean energy applications.

Declaration of competing interest

The author reported no potential conflict of interest.

Formatting of funding sources

There is no funding to declare.

References

[1] Bilgen, S., Structure and environmental impact of global energy consumption. Renewable and Sustainable Energy Reviews, 2014. 38: p. 890-902.
[2] Canbaz, C.H., et al., A Comprehensive Review and Status of Renewable Resources and Oil & Gas Under the Supply and Demand Dynamics in the World, in SPE Europec featured at 82nd EAGE Conference and Exhibition. 2021. p. D041S016R002.
[3] Shi, Q. and J. Wu, Review on Sulfur Compounds in Petroleum and Its Products: State-of-the-Art and Perspectives. Energy & Fuels, 2021. 35(18): p. 14445-14461.
[4] Shi, S., et al., Review on the Interaction Mechanism of Nitrogen/Sulfur Pollutants During Fuel Combustion. Journal of Energy Resources Technology, 2024. 146(10).
[5] Song, C., An overview of new approaches to deep desulfurization for ultra-clean gasoline, diesel fuel and jet fuel. Catalysis Today, 2003. 86(1): p. 211-263.
[6] Zbuzant, M., An Overview of the Use of Photo Catalysts for Desulfurization. Eurasian Journal of Chemical, Medicinal and Petroleum Research, 2022. 1(1): p. 10-19.
[7] Zhou, X., et al., Desulfurization through Photocatalytic Oxidation: A Critical Review. ChemSusChem, 2021. 14(2): p. 492-511.
[8] Zhang, Y., et al., Effective reduction of hydrogen consumption in ultra-deep hydrodesulfurization of diesel: Deep insights into the effect of thermodynamic limitations during hydrotreating. Fuel, 2024. 356: p. 129640.
[9] Kumar, S., S.V. Chandra, and S.M. and Nanoti, Extractive Desulfurization of Gas Oils: A Perspective Review for Use in Petroleum Refineries. Separation & Purification Reviews, 2017. 46(4): p. 319-347.

[10] Ismagilov, Z., et al., Oxidative Desulfurization of Hydrocarbon Fuels. Catalysis Reviews, 2011. 53(3): p. 199-255.
[11] Mikhail, S., T. Zaki, and L. Khalil, Desulfurization by an economically adsorption technique. Applied Catalysis A: General, 2002. 227(1): p. 265-278.
[12] Cano, P.I., et al., Life cycle assessment of different physical-chemical and biological technologies for biogas desulfurization in sewage treatment plants. Journal of Cleaner Production, 2018. 181: p. 663-674.
[13] Rajendran, A., et al., A comprehensive review on oxidative desulfurization catalysts targeting clean energy and environment. Journal of Materials Chemistry A, 2020. 8(5): p. 2246-2285.
[14] Boshagh, F., et al., Key Factors Affecting the Development of Oxidative Desulfurization of Liquid Fuels: A Critical Review. Energy & Fuels, 2022. 36(1): p. 98-132.
[15] Shafiq, I., et al., Efficient catalyst development for deep aerobic photocatalytic oxidative desulfurization: recent advances, confines, and outlooks. Catalysis Reviews, 2022. 64(4): p. 789-834.
[16] Dedual, G., et al., Requirements for effective photocatalytic oxidative desulfurization of a thiophene-containing solution using TiO2. Journal of Environmental Chemical Engineering, 2014. 2(4): p. 1947-1955.
[17] Li, F.-t., et al., Photocatalytic oxidative desulfurization of dibenzothiophene under simulated sunlight irradiation with mixed-phase Fe2O3 prepared by solution combustion. Catalysis Science & Technology, 2012. 2(7): p. 1455-1462.
[18] Yaqoob, A.A., et al. Advances and Challenges in Developing Efficient Graphene Oxide-Based ZnO Photocatalysts for Dye Photo-Oxidation. Nanomaterials, 2020. 10, DOI: 10.3390/nano10050932.
[19] Barba-Nieto, I., et al., Oxide-based composites: applications in thermo-photocatalysis. Catalysis Science & Technology, 2021. 11(21): p. 6904-6930.
[20] Alenazi, B., et al., Ionothermal Synthesis of Metal Oxide-Based Nanocatalysts and Their Application towards the Oxidative Desulfurization of Dibenzothiophene. Journal of Chemistry, 2020. 2020(1): p. 3894804.
[21] Sadrara, M. and M.K. Khorrami, Designing an efficient organic–inorganic hybrid nanocomposite for simultaneous oxidative/adsorptive desulfurization of model and real fuel oils. Scientific Reports, 2023. 13(1): p. 15134.
[22] Hitam, C.N.C. and A.A. Jalil, Recent advances on nanocellulose biomaterials for environmental health photoremediation: An overview. Environmental Research, 2022. 204: p. 111964.
[23] Mostafa, M.M., M. El saied, and A.S. Morshedy, Novel Calcium Carbonate-titania nanocomposites for enhanced sun light photo catalytic desulfurization process. Journal of Environmental Management, 2019. 250: p. 109462.
[24] Morshedy, A.S. and T. Mahmoud, Optimizing heavy crude oil conversion: Catalytic thermolysis with TiO2@α-Fe2O3 nanocomposite and surfactant dynamics. Petroleum, 2025. 11(2): p. 234-247.
[25] Bezrodna, T., et al., IR-analysis of H-bonded H2O on the pure TiO2 surface. Journal of Molecular Structure, 2004. 700(1): p. 175-181.
[26] León, A., et al. FTIR and Raman Characterization of TiO2 Nanoparticles Coated with Polyethylene Glycol as Carrier for 2-Methoxyestradiol. Applied Sciences, 2017. 7, DOI: 10.3390/app7010049.
[27] Sahai, A., et al., Cu/Cu2O/CuO nanoparticles: Novel synthesis by exploding wire technique and extensive characterization. Applied Surface Science, 2016. 390: p. 974-983.
[28] Habibi, M.H. and B. Karimi, Application of impregnation combustion method for fabrication of nanostructure CuO/ZnO composite oxide: XRD, FESEM, DRS and FTIR study. Journal of Industrial and Engineering Chemistry, 2014. 20(4): p. 1566-1570.
[29] Kumar, P.M., S. Badrinarayanan, and M. Sastry, Nanocrystalline TiO2 studied by optical, FTIR and X-ray photoelectron spectroscopy: correlation to presence of surface states. Thin Solid Films, 2000. 358(1): p. 122-130.
[30] Matthews, R.W. and S.R. McEvoy, A comparison of 254 nm and 350 nm excitation of TiO2 in simple photocatalytic reactors. Journal of Photochemistry and Photobiology A: Chemistry, 1992. 66(3): p. 355-366.
[31] Ando, M., et al., Optical CO sensitivity of Au–CuO composite film by use of the plasmon absorption change. Sensors and Actuators B: Chemical, 2003. 96(3): p. 589-595.
[32] El Sharkawy, H.M., M.A. Abo El-Khair, and A.S. Morshedy, Construction of SnS2@SnO2 nanocomposite Z-scheme heterojunction for dual-functional photocatalysis: Green hydrogen generation and crystal violet degradation. International Journal of Hydrogen Energy, 2025. 137: p. 471-486.
[33] Morshedy, A.S., et al., Highly efficient Imprinted Polymer Nanocomposites for photocatalytic desulfurization of real diesel fuel. Environmental Technology & Innovation, 2021. 21: p. 101206.
[34] Morshedy, A.S., et al., The production of clean diesel fuel by facile sun light photocatalytic desulfurization process using Cd-based diacetate as a novel liquid photocatalyst. Journal of Cleaner Production, 2021. 279: p. 123629.
[35] Koffyberg, F.P. and F.A. Benko, A photoelectrochemical determination of the position of the conduction and valence band edges of p-type CuO. Journal of Applied Physics, 1982. 53(2): p. 1173-1177.
[36] Wang, Z., et al., Recent Developments in p-Type Oxide Semiconductor Materials and Devices. Advanced Materials, 2016. 28(20): p. 3831-3892.
[37] Di Valentin, C., G. Pacchioni, and A. Selloni, Reduced and n-Type Doped TiO_2: Nature of Ti3+ Species. The Journal of Physical Chemistry C, 2009. 113(48): p. 20543-20552.
[38] Liu, C., et al., Crystal facet-dependent p-type and n-type sensing responses of TiO_2 nanocrystals. Sensors and Actuators B: Chemical, 2018. 263: p. 557-567.
[39] Li, H., et al., State-of-the-Art Progress in Diverse Heterostructured Photocatalysts toward Promoting Photocatalytic Performance. Advanced Functional Materials, 2015. 25(7): p. 998-1013.
[40] Xu, J., et al., Enhanced desulfurization performance of model fuel by Cu–ZnO/ TiO_2 heterostructure. RSC Advances, 2024. 14(49): p. 36733-36744.

[41] Jabbari, P., et al., Synthesis of Cu-doped TiO_2 modified $BiVO_4$ for photocatalytic oxidative desulfurization (PODS) of a model fuel. Journal of Photochemistry and Photobiology A: Chemistry, 2024. 452: p. 115625.
[42] Moeinifard, B. and A. Najafi Chermahini, Fabrication of Au-doped mesoporous TiO_2 supported on g-C3N4 as an efficient light-assisted catalyst for oxidative desulfurization of model fuels with different sulfur content. Journal of Materials Science: Materials in Engineering, 2025. 20(1): p. 14.
[43] Tiple, A., P.S. Sinhmar, and P.R. Gogate, Improved direct synthesis of TiO_2catalyst using sonication and its application for the desulfurization of thiophene. Ultrasonics Sonochemistry, 2021. 73: p. 105547.
[44] Zhu, W., et al., Photocatalytic oxidative desulfurization of dibenzothiophene catalyzed by amorphous TiO2 in ionic liquid. Korean Journal of Chemical Engineering, 2014. 31(2): p. 211-217.
[45] Anggraini, A., J. Jefri, and A. Lesbani, Efficient Desulfurization of 4-Methyldibenzothiophene Using H5PV2Mo10O40/TiO2: A Catalytic Approach. Indonesian Journal of Material Research, 2025. 3(1): p. 17-23.
[46] Song, Z., et al., Synthesis of TiO_2-Modified Y Zeolite and its Adsorption-Catalytic Oxidative Desulfurization Performance. Silicon, 2024. 16(10): p. 4159-4172.
[47] Morshedy, A.S., et al., Solar-powered commercial diesel fuel desulfurization: Exploring the factors affecting and recyclability of mesoporous Tl-doped TiO_2 nanofiber photocatalysts. Journal of Cleaner Production, 2024. 449: p. 141713.